Study of the antibacterial effects of chitosans on *Bacillus cereus* (and its spores) by atomic force microscopy imaging and nanoindentation

João C. Fernandes [a], Peter Eaton [b,*], Ana M. Gomes [a], Manuela E. Pintado [a], F. Xavier Malcata [a]

[a] *Escola Superior de Biotecnologia, Universidade Católica Portuguesa, Rua Dr. António Bernardino de Almeida, 4200-072 Porto, Portugal*
[b] *REQUIMTE, Departamento de Química, Faculdade de Ciências da Universidade do Porto, Rua do Campo Alegre, 4169-007 Porto, Portugal*

ARTICLE INFO

ABSTRACT

Bacillus cereus is a Gram-positive, spore-forming bacterium that is widely distributed in nature. Its intrinsic thermal resistance coupled with the extraordinary resistance against common food preservation techniques makes it one of the most frequent food-poisoning microorganisms causing both intoxications and infections. In order to control *B. cereus* growth/sporulation, and hence minimize the aforementioned hazards, several antimicrobial compounds have been tested. The aim of this work was to assess by atomic force microscopy (AFM) the relationship between the molecular weight (MW) of chitosan and its antimicrobial activity upon both vegetative and resistance forms of *B. cereus*. The use of AFM imaging studies helped us to understand how chitosans with different MW act differently upon *B. cereus*. Higher MW chitosans (628 and 100 kDa) surrounded both forms of *B. cereus* cells by forming a polymer layer—which eventually led to the death of the vegetative form by preventing the uptake of nutrients yet did not affect the spores since these can survive for extended periods without nutrients. Chitooligosaccharides (COS) (< 3 kDa), on the other hand, provoked more visible damages in the *B. cereus* vegetative form—most probably due to the penetration of the cells by the COS. The use of COS by itself on *B. cereus* spores was not enough for the destruction of a large number of cells, but it may well weaken the spore structure and its ability to contaminate, by inducing exosporium loss.

1. Introduction

Bacillus cereus is a very common culprit in food poisoning, causing both intoxications and infections [1]. This Gram-positive spore-forming bacterium is a common contaminant in a wide variety of foods, including milk and dairy products, cooked vegetables and meats, cereals (especially rice), among others [2,3]. Its thermo-resistance associated with the low sensitivity to the food preservation processes exhibited by its endospores makes *B. cereus* one of the major problems for the food industry [4,5]. In order to control *B. cereus* and hence minimize the aforementioned hazards, several antimicrobials have been tested as food additives [4,6]. However, there is a growing pressure on the food industry to reduce the use of synthetic chemical preservatives. Consequently, manufactures are urged to develop alternative preservatives that are based on natural compounds [6]. Chitosan is a natural non-toxic biopolymer derived by deacetylation of chitin, a major component of the exoskeletons of crustaceans and insects [6,7]. It has received considerable attention for its application in the biomedical, food, textile and chemical industries [6,8–10]. However, its high molecular weight (MW)—which causes high viscosity and low solubility in acid-free aqueous media—has limited its application [11]. Recent studies on chitosan have focused attention towards conversion to chitooligosaccharides (COS). These are water-soluble due to their shorter chain lengths (generally, the MW of COS is ⩽ 10 kDa) [12] and free amino groups in D-glucosamine units (which confer them positive charge that allow to bind strongly to negatively charged surfaces). Additionally, they have been reported to possess versatile functional properties that make them a very promising class of compounds, e.g. antitumor activity, immuno-enhancing effects, enhancement of protection against infection by some pathogens, as well as antifungal and antibacterial activities [13–16].

Atomic force microscopy (AFM) is a highly suitable tool for the study of bacteria, and has been widely applied to such samples not only for imaging but also for probing other properties of bacteria as well [17–23]. A great advantage of AFM is that samples do not require fixation, conductive coating, or to be imaged under vacuum conditions. Furthermore, samples may be imaged in pseudo-physiological conditions, i.e. in buffer or growth medium, and this has been applied to image hydrated bacteria [20]. However, images of bacteria in liquid often show reduced topographical contrast compared to images in air-dried samples, and features such as flagelli can be absent in these images [17,20,24].

* Corresponding author. Tel.: +351 22 040 2585; fax: +351 22 040 2659.
E-mail address: peter.eaton@fc.up.pt (P. Eaton).

Applications of AFM imaging studies on bacteria include imaging of bacterial nanostructures [17,25–27], genetic variation [28,29], and the study of antibacterial effects [28,30–32]. The extremely high resolution of AFM allows the imaging of features as small as 3 nm rodlets on bacterial endospores [27], making AFM extremely advantageous for the determination of small highly delicate structures on bacteria. A recent study combining confocal laser scanning and atomic force microscope [25] has shown to be useful to examine environmental bacterial samples, and identify and measure bacterial nanostructures within them. Assessment of damage to bacteria by control agents includes the morphological changes to *Escherichia coli* caused by the antibiotic defodizime [30], *Staphylococcus aureus* response to vancomycin [28], and also *E. coli* response to antibacterial peptides [31]. The antimicrobials' damage includes collapsing of cells, appearance of holes, and surface roughening on cells. AFM has been used to assess the morphological changes on *E. coli* after treatment with copper-loaded chitosan nanoparticles [33]. Unfortunately, the resulting images lost all similarity to bacterial morphology and were hard to interpret.

We recently published data comparing AFM observations of antimicrobial effects on Gram-positive and Gram-negative bacteria (namely *E. coli* and *S. aureus*) by chitosan and COS [34]. The morphological analysis showed that the COS induced clustering in *E. coli*, and some cell collapse, whereas when treated by the high molecular weight chitosan, the cells stayed separate, and a much larger proportion showed cell damage or collapse. Interestingly, neither compound had a great effect upon the morphology of *S. aureus.* In order to clarify the effect of the polymers on the two species, the AFM was used to carry out nanoindentation analysis on them.

This last mentioned technique is a member of the class of non-imaging modes made possible with the AFM. This also includes force spectroscopy, in which the behaviour of the AFM tip as it is withdrawn from the sample is monitored. This is highly sensitive to the nature of the tip–sample interaction [35]. For example, *Acinetobacter venetianus* and *Rhodococcus erythropolis* were examined with hydrophilic and hydrophobic tips to characterise the heterogeneity in bacterial surface hydrophobicity by measuring force spectroscopic data (acquisition of force–distance curves) [22]. The adhesion in the force curves was plotted as a function of cell surface location, to get an idea whether hydrophilic/hydrophobic patches were present. In the case of *R. erythropolis*, larger forces were seen at one end of the rod-like bacteria than at the other, and this was attributed to asymmetry induced on cell division.

If instead of analysing the part of the force–distance curve where the AFM tip withdraws from the surface, one analyses the approach and subsequent bending in contact of the tip on the surface, it is possible to extract mechanical information about the sample from the force curve [36–39].

This approach has been used to measure the turgor pressure of bacteria by measuring dynamic compliance using the AFM tip oscillating at 14 Hz [40,41]. When the tip indents into the sample surface (i.e. the bacterium), this technique is called nanoindentation. Gaboriaud et al. [21] have performed spatially resolved nanoindentation by force–distance curve mapping across the surface of *Shewanella putrefaciens*, and showed that the data fit well to a Hertzian mechanical model, which revealed that the surface possessed more elastic behaviour in the centre of the cell and was more plastic at the edge of the cell. However, measurements of such curves on the cell edge are liable to geometric difficulties [18,37]. Using such models as the Hertz model, it is possible, at least in principle, to determine from nanoindentation measurements real physical parameters, such as cell stiffness, or Young's modulus (E) of the probed cells [19,39,42]. As mentioned previously [34], this sort of analysis only gives really an estimate of Young's modulus, due to assumptions made about certain experimental conditions that are not usually known, but the results produced by different research groups point to typical values of E of the order of 10^2–10^3 MPa for (vegetative) bacterial cells [17,34].

This communication describes the application of AFM imaging to study the antimicrobial effect of chitosans and chitooligosaccharides on both types of *B. cereus* cells—vegetative and spore. The results are correlated with cell-viability studies, and help us understand how the bacteria react to the treatment by different polymers. In addition, nanoindentation of the bacterial cells is used to assess the effect of the chitooligosaccharides on cell rigidity.

2. Experimental

2.1. Chitosans and microorganisms

Chitosans with average molecular weight 628 and 100 kDa (degree of deacetylation: 80–85%) were purchased from Sigma-Aldrich. Chitooligosaccharide mixture was purchased from Nice-chem (Shanghai, China) with molecular weight <3 kDa. For the preparation of the chitosan solution, the as-received chitosan was dissolved in 0.5% (v/v) acetic acid to make a 2.5% (w/v) solution. Similarly, the COS was dissolved in water to 2.5% (w/v). In both cases, the pH was adjusted to 5.8 with 10 M NaOH. After stirring overnight, the solutions were autoclaved at 120 °C for 15 min. Microorganisms were purchased from ATCC, *B. cereus* (ATCC 14579).

2.2. Spore production

Cells were precultivated at 37 °C for 24 h in Brain Heart Infusion (Difco) medium. The preculture was used to inoculate nutrient agar plates (Biokar Diagnostics BK021) to which were added MnSO$_4$ 40 mg/L and CaCl$_2$ 100 mg/L to encourage sporulation. Plates were incubated at 30 °C for 7 days. Spores were then collected by scraping the surface of the agar and suspended in sterile phosphate buffer M/15 at pH 7 and washed three times by centrifugation (10,000g for 15 min). The pellet was then resuspended in 5 ml distilled water and 5 ml ethanol. The suspension obtained was kept at 4 °C for 12 h in order to eliminate vegetative nonsporulated bacteria and washed again three times by centrifugation in distilled water. Lastly, the final suspension (about 10^{10} spores per mL) was distributed in sterile Eppendorf microtubes and kept at 4 °C.

2.3. Assays for antimicrobial activity

Antimicrobial activity of the two chitosans and the COS was tested against both types of *B. cereus* cells—vegetative and spore—in Muller-Hinton broth using inocula of ca. 10^8–10^9 cells/mL. This was done by adding solutions of chitosan or COS to reach a final concentration of 0.50, 0.25 or 0.10% (w/v). After fixed treatment times of 0, 1, 2 or 4 h of incubation at 37 °C, 1 mL of each sample was diluted and plated by the spread technique on Plate Count Agar (Lab M). The plates were incubated at 37 °C for 24 h and the viable cell numbers determined. Triplicate analyses of each sample were performed and each experiment was carried out in duplicate.

2.4. Preparation and analysis of AFM samples

The effect of the compounds on the bacterial cell surfaces was examined by AFM. Samples were prepared by applying 40 μL of bacterial suspension without treatment (control) or treated with COS or chitosan onto a clean glass surface, followed by air-drying. The samples were incubated in the presence of COS or chitosan for the same treatment times as for the antimicrobial assays. The samples were then gently rinsed with deionized water to remove salt crystals, and air-dried again before analysis. Samples were examined within 24 h of deposition; previous work showed that although the samples were air-dried, further dehydration could change cell morphology if the cells were examined after extended periods (>1 week) in a dry condition. The samples were dried under ambient conditions; no special care was taken over the drying conditions; however, all samples were prepared at the same time and so were exposed to the same conditions.

AFM was carried out with a Veeco Multimode IVa atomic force microscope (Veeco, Santa Barbara, CA), equipped with a j-type scanner (ca. $100 \times 100 \times 5 \, \mu m^3$ scan range). Bacterial morphology studies were carried out in tapping mode in air, using fresh silicon cantilevers with a resonant frequency approximately 300 kHz (AppNano, Santa Clara, CA, USA). Two independently prepared samples were analyzed, and several different areas were studied on each sample, but only characteristic images are shown here. For nanoindentation experiments, the samples were first scanned in tapping mode to identify suitable cells. In each case, cells that appeared to be intact were chosen for analysis. Nanoindentation was then performed in the contact mode, firstly on the glass slide surface, to calibrate detector sensitivity, and then in the centre of the selected bacteria. The nanoindentation experiments were carried out with the same type of probe as those used for imaging; the spring constant of these cantilevers was nominally 40 N/m. The cantilever chosen for these experiments was rather stiffer than used elsewhere for studies of hydrated microorganisms in liquid [37,43], but only slightly more stiff than that used in our previously reported work on bacterial cells [34]. This was chosen due to the higher cell rigidity in air, and the well-known high rigidity of bacterial spores [44]. Areas within the centre of each cell were selected for analysis and at least 49 force curves were measured for each cell. Three or more cells were analyzed for each condition. The data were averaged during analysis. Measurements were repeated with bacteria grown and treated separately and with a different AFM cantilever to check for reproducibility; however, all data presented here were generated with the same cantilever. Analysis of the curves on the basis of the Hertz model was carried out with PUNIAS software (P. Carl, P. Dalhaimer) [45], using the sphere model of the tip using the nominal tip radius of 10 nm and the nominal spring constant.

3. Results and discussion

Morphological characterization of the control *B. cereus* vegetative cells samples observed in Fig. 1 showed typically rod-shaped cells with smooth surfaces (the dimension of these cells was around 350–650 nm height, and 3.5–4.0 μm in length). Often the cells also showed many pili or fimbria, typically extended on the glass surface. The top-left image in Fig. 1 is a typical area showing a group of untreated vegetative cells. Pan and co-authors also reported similar cell structure such as the shape and size [46]. Fig. 1 (left) shows images from samples treated for 4 h with COS at 0.25% and 0.50% (w/v). Both images exhibit several differences when compared with the control bacteria regarding the cell structure: cells collapsed and became rougher; the pili or fimbria seen in the control were not seen after COS treatment. However,

there were also apparently undamaged cells seen in all samples (e.g. as shown on the bottom left image—0.50% (w/v)). After all COS treatments a range of cell morphologies were observed, ranging from severely damaged cells, through cells with light damage, to cells very similar to the control cells. The images on the right of Fig. 1 show the response of *B. cereus* spores after they were exposed to the same conditions described above for vegetative cells. Untreated spores (Fig. 1, top right) were found to be slightly elongated (1500–2000 nm long, 900–1150 nm wide and 800–1090 nm high). Some irregular features observed on the spore surfaces were described previously as grooves, bumps or grain-like features by Zolock et al. [47]. In the control sample we also saw some structures surrounding the spores that closely resembled a loose layer of exosporium, as previously described [48,49]—a protective layer that surrounds the spore protecting the core of DNA, and which we observed generally spread out on the surface. The loss of the exosporium was even more apparent at the highest COS concentration used (bottom right). We also noted that in the morphological studies, the spores treated with 0.5% COS had somewhat lower heights (958 ± 71 nm) than the control spores (990 ± 51 nm), which might be related to exosporium loss. In fact, this was the only change clearly demonstrated by AFM imaging concerning the treatment of *B. cereus* spores with COS. The use of COS at the concentrations tested did not appear to affect the spore integrity: the shape and size seemed to be unaffected, as well as the spore cell wall. However, the loss of the exosporium, which influences spore hydrophobicity and organism pathogenicity, may play an important role, not in the cell germination process by itself [50], but in resistance to other chemical/thermal treatments [51] or in its ability to colonize a surface or a host.

Fig. 2 shows the images of *B. cereus* vegetative cells treated with 0.10% (w/v) of 100 (left) and 628 (right) kDa chitosans. We found that the cells were harder to resolve than with the COS, even at this low concentration, as they were covered in a thick layer of the polymer. Confocal microscopy showed that the material surrounding the cells was indeed chitosan (unpublished results). In fact, the coating of the cells with a hard-to-remove polymer layer may well be the mode of action of high molecular weight chitosans on bacteria [34,52]. Similar effects were seen when imaging the spores exposed to these chitosans (Fig. 3). Furthermore, for the higher MW chitosan it was harder to resolve the spores: in the left image (100 kDa chitosan) it is still possible to recognize some of the features observed on the control sample, such as the vein-like features on the surface. However, with the 628 kDa chitosan we can only distinguish the spore shape. Overall, it was not clear from the morphological studies alone whether the lack of visible changes in the case of the spores meant that less damage was suffered by them, or if it only meant that due to greater mechanical resistance, the spores exhibited less morphological change after chitosan or COS action than the vegetative cells.

In order to clarify these results, it was decided to carry out nanoindentation studies on the treated and untreated cells to ascertain whether the polymer exposure affected the mechanical strength of the cells. As described in the introduction, this technique can provide stiffness measurements of the surface of individual cells, which can be sensitive to factors such as treatment or the bacterial strain [38,42,53]. Only cells conforming to the normal bacterial gross morphology (rod-like for vegetative cells, rice grain-shaped for spores) and of similar dimensions to those in the control were examined, although other features that may have greatly distorted cells were sometimes observed in the treated samples. Care was taken to ensure that all measurements were made on the highest part of the cell, i.e. that where the cell wall would be perpendicular to the motion of the cantilever, as it is known that geometric effects can change the measured stiffness
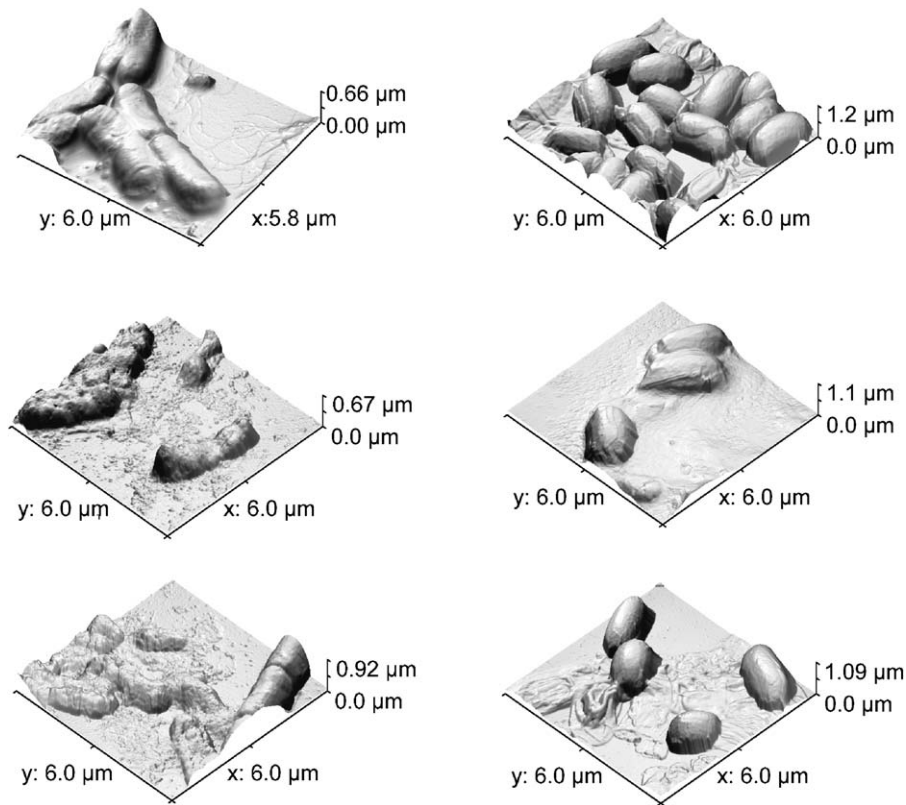
Fig. 1. Tapping mode AFM images of the effect of COS on cell morphology. Left: cells of *B. cereus*, right: spores of *B. cereus*. Top: control with no COS, middle: after exposure to 0.25% (w/v) COS, bottom: after exposure to 0.50% (w/v) COS.
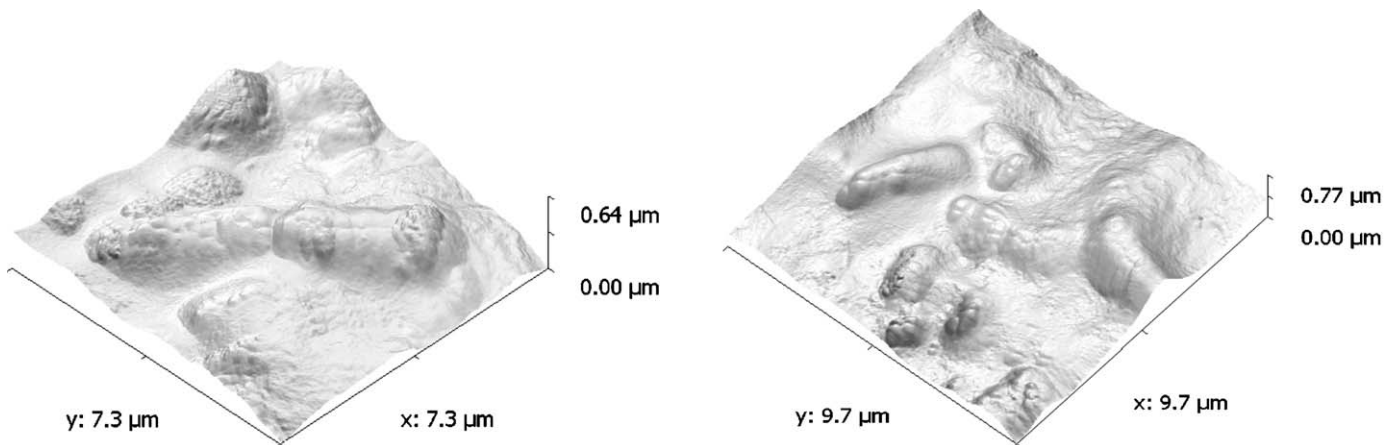
Fig. 2. Tapping mode AFM images of vegetative cells of *B. cereus* exposed to 0.10% (w/v) of 100 kDa (left) and 600 kDa chitosan (right).

when comparing the edges to the centre of the cell [18,37]. Data were later averaged for analysis. It was decided to apply this technique only to study bacteria treated by COS as the imaging studies had clearly shown chitosan-treated bacteria and spores coated with a layer of polymer, which would mean that nanoindentation would probe the polymer rather than the bacteria. Attempts to remove the polymer film by washing were unsuccessful. Untreated cells were studied as a control, and compared to cells treated for 4 h by 0.10%, 0.25% or 0.50% (w/v) COS. The averaged results from the fitting to the nanoindentation data are shown for both types of *B. cereus* cells in Table 1, and example data are shown in Fig. 4.

It may be observed that the values of Young's modulus (*E*) attained were quite different between vegetative and spore cells. This was also reflected in the slopes of the raw data (Fig. 4). The control spores were more than five times stiffer than the control bacteria. Although mechanical rigidity of spores compared to the mother cells is well known [44], to the best of our knowledge it has never been directly shown in this way before. Overall, the spores decreased somewhat in cell rigidity with increasing COS concentration, especially so at 0.5% (w/v) concentration, while still being considerably stiffer than vegetative cells under all conditions. This presumably reflects the weakening of the spore wall due to the loss of the exosporium (visible in Fig. 1) and
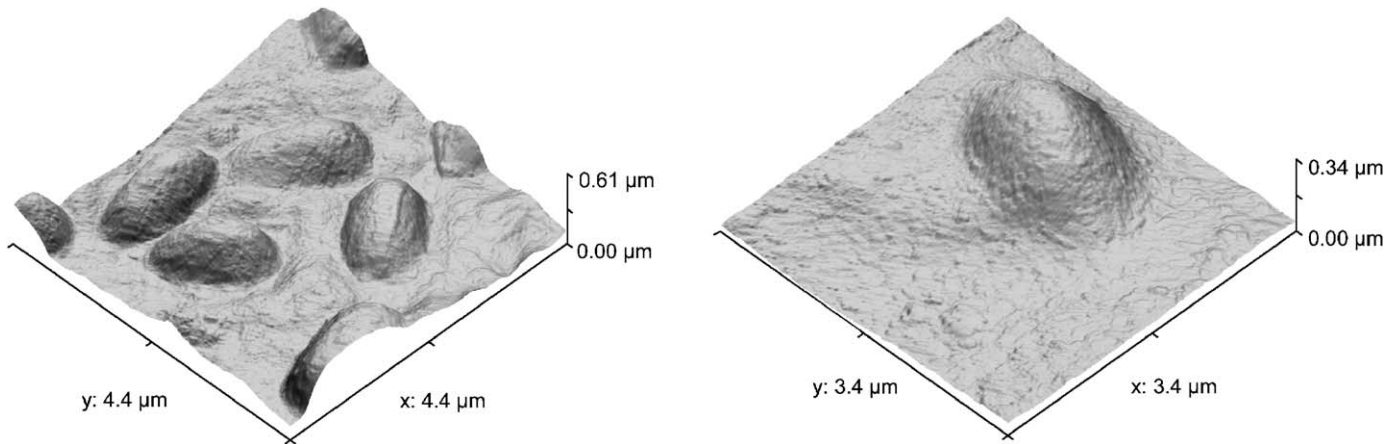
Fig. 3. Tapping mode AFM images of spores of *B. cereus* exposed to 0.10% (w/v) of 100 kDa (left) and 600 kDa chitosan (right).

Table 1
Results of Hertzian mechanics fitting to mean nanoindentation curves measured on untreated (control) cells or cells treated for 4 h with different concentrations of chitooligosaccharide (COS)-average ± standard deviation.

	Vegetative cells (MPa)	Spores (MPa)
Control	834 ± 479	4391 ± 1516
0.10% (w/v)	1073 ± 577	3901 ± 1136
0.25% (w/v)	639 ± 491	3901 ± 994
0.50% (w/v)	1174 ± 855	2264 ± 1403

perhaps other inner protective layers. On the other hand, the average results on the *B. cereus* vegetative cells showed no particular trend in cell rigidity versus concentration of COS, and more variability was observed, based on the larger values of standard deviation. This contrasts with the AFM imaging results, which showed considerable morphological changes in *B. cereus* after exposure to COS (Fig. 1). A reason for the variable nanoindentation results may be that the effects of COS upon different individual cells varied widely. Fig. 5 illustrates two different cells from the same sample; one cell was considerably affected in cell shape (right cell), and also considerably less rigid according to the nanoindentation results. Table 1 shows that for treatment with 0.25% and 0.5% (w/v) COS, the standard deviation values of the stiffness of the vegetative cells were almost the same as the mean values, indicating huge variability in cell stiffness under these conditions. This variability could reflect the fact that once the COS entered the vegetative cells, damage was rapid, whereas the presence of COS outside the cells had little effect. Another possibility is that the dehydration level affected the cell rigidity in a very variable way; this would presumably have less effect on the more resistant spores. It would be interesting to study the effect of these treatments on hydrated spores and cells and compare the results to those reported here. Comparison between dehydrated and hydrated cell stiffness is currently lacking in the literature. We plan to carry out this work in the future.

Comparing the data of these two forms of *B. cereus*, vegetative cells possessed comparable stiffness to previously studied bacteria [34], while the spores were consistently and considerably stiffer than any of the bacteria studied so far, but similar in stiffness to spores of *Aspergillus nidulans* [27]. Such mechanical rigidity is likely related to their increased resistance to mechanical, thermal, or chemical attack versus the bacteria in the vegetative form as previously discussed [54]. Repeatability studies
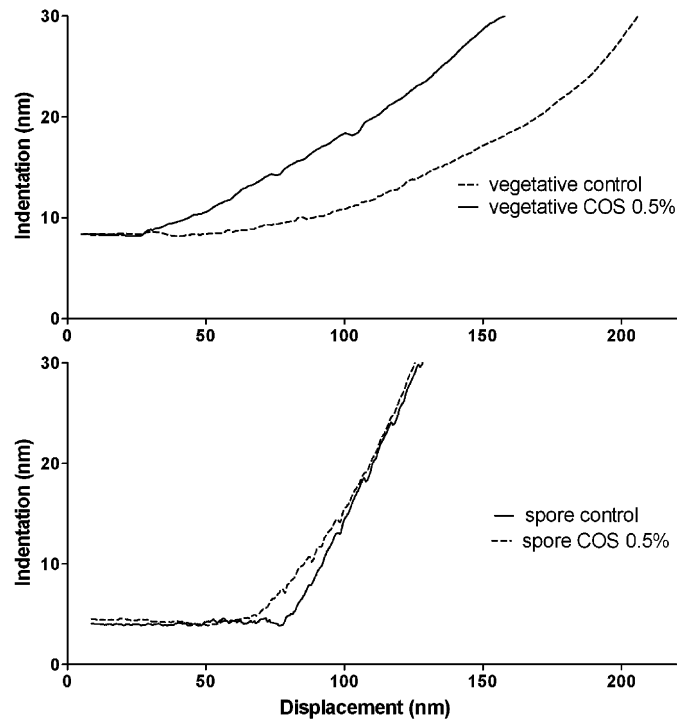
Fig. 4. Example of nanoindentation data (deflection–distance curves) showing results from control and 0.5% COS-treated vegetative (top) and spore (bottom) *B. cereus* cells.
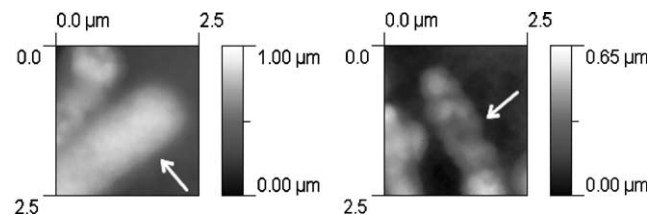
Fig. 5. Details of AFM images showing variability of *B. cereus* vegetative cells exposed to 0.10% (w/v) COS. The arrowed cell on the left had a Young's modulus value of 1490 MPa, the right cell had 594 MPa.

with a different cantilever showed similar results, with somewhat different values of Young's modulus as expected due to the assumptions made about probe tip radius and spring constant.

It is instructive to compare the data obtained from the AFM experiments already described to those obtained by standard cell-counting studies. The results of cell-viability studies on both types of *B. cereus* cells, using both COS and chitosan, are presented in Fig. 6. In the case of the vegetative cells (Fig. 6a), the chitosan with 628 kDa reduced the number of viable cells by almost 3 orders of magnitude within the first 4 h. In fact, after the 4 h period this was the only compound that presented bactericidal action (defined as a reduction of 3 cycles log in CFUs). Both COS and 100 kDa chitosan led to lower reduction levels of the initial cell population. Overall, the different levels of reduction attained by the compounds with different MW suggest that the longer polymer chains give stronger antibacterial action on the *B. cereus* vegetative cells. The comparison of these data to the observations made by AFM allows us to understand the possible mode of action more clearly. In the case of COS, some of the cells appeared to be collapsed. This effect may be due to penetration of the cells by COS, facilitated by its small size, as suggested previously in works applied to different species [34,52,55]. It was suggested that this would lead to disruption of the cell wall and/or flocculation of the negatively charged molecules inside the bacterium such as DNA or some proteins, since COS is in a protonated form under physiological conditions [56,57]. However, for the 628 and 100 kDa chitosans, due to their greater chain length, the molecules did not penetrate the cell. Instead, apparently these molecules formed a polymer layer surrounding the cell, creating a barrier to metabolite transport that eventually led to cell death due to the lack of nutrients [34,52].

According to the data presented in Fig. 5, this mechanism is more effective against the vegetative cells than that promoted by COS. Analysing the results for *B. cereus* spores, neither of the chitosans showed any effect upon them, showing a negligible reduction in number of colony forming units (Fig. 6b). Based on the presumed method of action of chitosan described above, preventing nutrient absorption by spores had no effect. It has been reported that spores can survive for centuries without any nutrients, which explains the absence of any reduction on spore viable numbers. Regarding COS, the reduction achieved was around 1-log cycle (ca. 90%), which although higher than that produced by chitosans, for an antimicrobial agent is considered a very low reduction level. Once again, based on the postulated method of action of COS, it appears to be very difficult for COS to penetrate in the spores, presumably due to the strength derived from the several protective coats that surround the cell and that make endospores the most resistant living structures known [44,58]. As supported by AFM images, spore cells did not seem to be destroyed or to collapse due to COS as seen for vegetative cells, instead they only seemed to lose their external layer—exosporium, which is not essential for the germination process (thus not affecting spore viable numbers to a great extent). However, this action may lead to a weakening of the spore structure, as shown by the indentation measurements, since the exosporium has been described as being associated with spore resistance to several chemical and thermal treatments [51,59,60] and also with its ability to contaminate surfaces [61,62]. The method of action of the COS cannot be definitively determined from the data presented here; however, it is clear that the overall structure of the spores was little affected by the action of the COS in comparison to the action on the vegetative cells (compare the images in the left column and the right column of Fig. 1).

4. Conclusion

The use of AFM imaging studies provided a useful tool to understand how chitosans with different MW act differently upon *B. cereus*. Higher MW chitosans (628 and 100 kDa) surrounded both forms of *B. cereus* by forming a polymer layer—which eventually led to the death of the vegetative form by preventing the uptake of nutrients but did not affect the spores since these can survive for extended periods without the access to nutrients. On the other hand, COS (<3 kDa) induced more visible damages in the *B. cereus* vegetative form—most probably due to the penetration of the cells by the COS. The use of COS by itself on *B. cereus* spores was not enough for the destruction of a large number of cells, but it may weaken the spore structure and its ability to contaminate, by inducing exosporium loss.

Acknowledgments

Fig. 6. Enumeration of viable cell numbers (CFU/mL) for *B. cereus* vegetative cells (a) and *B. cereus* spores (b), treated with COS or chitosan at 0.50% (w/v)—average ± standard deviation.

help with the PUNIAS software. The authors thank two anonymous referees for their valuable contributions to the discussion of the data.

References

[1] Y.L. Liu, B. Elsholz, S.O. Enfors, M. Gabig-Ciminska, Journal of Microbiological Methods 70 (1) (2007) 55.
[2] J.E. Reyes, J.M. Bastias, M.R. Gutierrez, M.D.O. Rodriguez, Food Microbiology 24 (1) (2007) 1.
[3] L.P.S. Arnesen, K. O'Sullivan, P.E. Granum, International Journal of Food Microbiology 116 (2) (2007) 292.
[4] A.M. Abdou, S. Higashiguchi, A.M. Abouleinin, M. Kim, H.R. Ibrahim, Food Control 18 (2) (2007) 173.
[5] L.M. Hornstra, P.L.A. de Leeuw, R. Moezelaar, E.J. Wolbert, Y.P. de Vries, W.M. de Vos, T. Abee, International Journal of Food Microbiology 116 (3) (2007) 367.
[6] F. Devlieghere, L. Vermeiren, J. Debevere, International Dairy Journal 14 (4) (2004) 273.
[7] M. Rinaudo, Progress in Polymer Science 31 (7) (2006) 603.
[8] H.K. No, N.Y. Park, S.H. Lee, S.P. Meyers, International Journal of Food Microbiology 74 (1-2) (2002) 65.
[9] C. Shi, Y. Zhu, X. Ran, M. Wang, Y. Su, T. Cheng, Journal of Surgical Research 133 (2) (2006) 185.
[10] S.H. Lim, S.M. Hudson, Carbohydrate Polymers 56 (2) (2004) 227.
[11] A.B.V. Kumar, M.C. Varadaraj, R.G. Lalitha, R.N. Tharanathan, Biochimica et Biophysica Acta—General Subjects 1670 (2) (2004) 137.
[12] S.K. Kim, N. Rajapakse, Carbohydrate Polymers 62 (4) (2005) 357.
[13] K. Suzuki, T. Mikami, Y. Okawa, A. Tokoro, S. Suzuki, M. Suzuki, Carbohydrate Research 151 (1986) 403.
[14] A. Tokoro, N. Tatewaki, K. Suzuki, T. Mikami, S. Suzuki, M. Suzuki, Chemical & Pharmaceutical Bulletin 36 (2) (1988) 784.
[15] K. Tsukada, T. Matsumoto, K. Aizawa, A. Tokoro, R. Naruse, S. Suzuki, M. Suzuki, Japanese Journal of Cancer Research: Gann 81 (3) (1990) 259.
[16] Y. Uchida, M. Izume, A. Ohtakara, in: T. Skjak-Bræk, T. Anthonsen, P. Sandford (Eds.), Chitin and Chitosan: Sources, Chemistry, Biochemistry, Physical Properties, and Applications, Elsevier, London, UK, 1989, p. 373.
[17] A.V. Bolshakova, O.I. Kiselyova, I.V. Yaminsky, Biotechnology Progress 20 (6) (2004) 1615.
[18] C.J. Wright, I. Armstrong, Surface and Interface Analysis 38 (11) (2006) 1419.
[19] W.R. Bowen, R.W. Lovitt, C.J. Wright, Biotechnology Letters 22 (11) (2000) 893.
[20] M.J. Doktycz, C.J. Sullivan, P.R. Hoyt, D.A. Pelletier, S. Wu, D.P. Allison, Ultramicroscopy 97 (1-4) (2003) 209.
[21] F. Gaboriaud, S. Bailet, E. Dague, F. Jorand, Journal of Bacteriology 187 (11) (2005) 3864.
[22] L.S. Dorobantu, S. Bhattacharjee, J.M. Foght, M.R. Gray, Langmuir 24 (9) (2008) 4944.
[23] Z. Suo, X. Yang, R. Avci, L. Kellerman, D.W. Pascual, M. Fries, A. Steele, Langmuir 23 (3) (2007) 1365.
[24] P. Schaer-Zammaretti, J. Ubbink, Ultramicroscopy 97 (1-4) (2003) 199.
[25] T. Schmid, J. Burkhard, B.S. Yeo, W.H. Zhang, R. Zenobi, Analytical and Bioanalytical Chemistry 391 (5) (2008) 1899.
[26] A. da Silva, O. Teschke, World Journal of Microbiology & Biotechnology 21 (6–7) (2005) 1103.
[27] L.M. Zhao, D. Schaefer, M.R. Marten, Applied and Environmental Microbiology 71 (2) (2005) 955.
[28] S. Boyle-Vavra, J. Hahm, S.J. Sibener, R.S. Daum, Antimicrobial Agents and Chemotherapy 44 (12) (2000) 3456.
[29] S.E. Cross, J. Kreth, L. Zhu, F.X. Qi, A.E. Pelling, W.Y. Shi, J.K. Gimzewski, Nanotechnology 17 (4) (2006) S1.
[30] P.C. Braga, D. Ricci, Antimicrobial Agents and Chemotherapy 42 (1) (1998) 18.
[31] M. Meincken, D.L. Holroyd, M. Rautenbach, Antimicrobial Agents and Chemotherapy 49 (10) (2005) 4085.
[32] I.B. Beech, J.R. Smith, A.A. Steele, I. Penegar, S.A. Campbell, Colloids and Surfaces B—Biointerfaces 23 (2–3) (2002) 231.
[33] W.L. Du, Y.L. Xu, Z.R. Xu, C.L. Fan, Nanotechnology 19 (8) (2008).
[34] P. Eaton, J.C. Fernandes, E. Pereira, M.E. Pintado, F.X. Malcata, Ultramicroscopy 2008 (2008).
[35] N.A. Burnham, H.M. Colton, H.M. Pollock, Nature 4 (1993) 64.
[36] N.A. Burnham, R.J. Colton, Journal of Vacuum Science and Technology A 7 (4) (1989) 2906.
[37] S.B. Velegol, B.E. Logan, Langmuir 18 (13) (2002) 5256.
[38] M.A. Beckmann, S. Venkataraman, M.J. Doktycz, J.P. Nataro, C.J. Sullivan, J.L. Morrell-Falvey, D.P. Allison, Ultramicroscopy 106 (8–9) (2006) 695.
[39] A. Vinckier, G. Semenza, FEBS Letters 430 (1998) 12.
[40] W. Xu, P.J. Mulhern, B.L. Blackford, M.H. Jericho, I. Templeton, Scanning Microscopy 8 (3) (1994) 499.
[41] X. Yao, J. Walter, S. Burke, S. Stewart, M.H. Jericho, D. Pink, R. Hunter, T.J. Beveridge, Colloids and Surfaces B—Biointerfaces 23 (2-3) (2002) 213.
[42] J. Wang, S. He, S. Xie, L. Xu, N. Gu, Materials Letters 61 (3) (2007) 917.
[43] G. Francius, B. Tesson, E. Dague, V. Martin-Jézéquel, Y.F. Dufrêne, Nanostructure and nanomechanics of live Phaeodactylum tricornutum morphotypes, Environmental Microbiology 10 (2008) 1344.
[44] P. Setlow, in: G. Storz, R. HenggeAronis (Eds.), Bacterial Stress Responses, Amer Soc Microbiology, Washington, 2000, p. 217.
[45] P. Carl, C.H. Kwok, G. Manderson, D.W. Speicher, D.E. Discher, Proceedings of the National Academy of Sciences of the United States of America 98 (4) (2001) 1565.
[46] J. Pan, X. Ge, R. Liu, H. Tang, Colloids and Surfaces B: Biointerfaces 52 (1) (2006) 89.
[47] R.A. Zolock, G.M. Li, C. Bleckmann, L. Burggraf, D.C. Fuller, Micron 37 (4) (2006) 363.
[48] P. Gerhardt, E. Ribi, Journal of Bacteriology 88 (6) (1964) 1774.
[49] O. Tarasenko, S. Lone, P. Alusta, Carbohydrate Research 343 (13) (2008) 2243.
[50] M. Plomp, T.J. Leighton, K.E. Wheeler, H.D. Hill, A.J. Malkin, Proceedings of the National Academy of Sciences of the United States of America 104 (23) (2007) 9644.
[51] A.O. Henriques, C.P. Moran, Annual Review of Microbiology 61 (2007) 555.
[52] L.-Y. Zheng, J.-F. Zhu, Carbohydrate Polymers 54 (4) (2003) 527.
[53] I. Penegar, C. Toque, S.D.A. Connell, J.R. Smith, S.A. Campbell, Additional Papers from the 10th International Congress on Marine Corrosion and Fouling, 2001.
[54] A.C. Lopez, A.M. Alippi, International Journal of Food Microbiology 117 (2) (2007) 175.
[55] C. Qin, H. Li, Q. Xiao, Y. Liu, J. Zhu, Y. Du, Carbohydrate Polymers 63 (3) (2006) 367.
[56] X.F. Liu, Y.L. Guan, D.Z. Yang, Z. Li, K.D. Yao, Journal of Applied Polymer Science 79 (7) (2001) 1324.
[57] J.C. Fernandes, F.K. Tavaria, J.C. Soares, Ó.S. Ramos, M. João Monteiro, M.E. Pintado, F. Xavier Malcata, Food Microbiology 25 (7) (2008) 922.
[58] A. Atrih, S.J. Foster, Antonie van Leeuwenhoek, International Journal of General and Molecular Microbiology 75 (4) (1999) 299.
[59] M.J. Johnson, S.J. Todd, D.A. Ball, A.M. Shepherd, P. Sylvestre, A. Moir, Journal of Bacteriology 188 (22) (2006) 7905.
[60] J.M. Daubenspeck, H.D. Zeng, P. Chen, S.L. Dong, C.T. Steichen, N.R. Krishna, D.G. Pritchard, C.L. Turnbough, Journal of Biological Chemistry 279 (30) (2004) 30945.
[61] C. Faille, G. Tauveron, C.L. Gentil-Lelievre, C. Slomianny, Journal of Food Protection 70 (2007) 2346.
[62] G. Tauveron, C. Slomianny, C. Henry, C. Faille, International Journal of Food Microbiology 110 (3) (2006) 254.